

Uncertainty in hydromorphological and ecological assessments of lowland river floodplains resulting from land cover classification errors

Menno W. Straatsma^{1,7}, Marcel van der Perk^{2,6}, Aafke M. Schipper^{3,6}, Reinier J.W. de Nooij⁴, Rob S.E.W. Leuven^{3,6}, Fredrik Huthoff⁵, Hans Middelkoop^{2,6}.

¹ Department of Earth System Analysis, Faculty of Geo-Information Science and Earth Observation (ITC), University of Twente,
PO Box 6, 7500 AA Enschede, the Netherlands,
straatsma@itc.nl, tel. +31 (0)53 4874245, fax +31 (0)53 4874336

² Faculty of Geosciences, Department of Physical Geography, Utrecht University,
PO Box 80115, 3508 TC Utrecht, The Netherlands,
m.vanderperk@geo.uu.nl, h.middelkoop@geo.uu.nl

³ Radboud University Nijmegen, Institute for Wetland and Water Research, Department of Environmental Sciences
PO Box 9010, 6500 GL Nijmegen, The Netherlands,
a.schipper@science.ru.nl, r.leuven@science.ru.nl

⁴ Optimal Planet training and consultancy,
P.O. Box 9010, 6500 GL, Nijmegen,
reinier.denooij@gmail.com

⁵ Water systems modelling, HKV Consultants,
PO Box 2120, 8203 AC Lelystad, the Netherlands,
f.huthoff@hkv.nl

⁶ NCR, Netherlands Centre of River Research, Delft, The Netherlands

⁷ Corresponding author

Abstract

Land cover maps provide essential input data for a sequence of models used to assess the hydromorphological and ecological aspects of lowland rivers and their floodplains, but the effect of land cover classification errors on these models has not been quantified in an integrated way. Our main objective is to assess the uncertainty in hydromorphological and ecological modeling of a large lowland river depending on the classification accuracy (CA) of a land cover map. We quantified the uncertainty for the three distributaries of the river Rhine in The Netherlands with respect to four aspects: (1) hydrodynamics, (2) annual average suspended sediment deposition, (3) ecotoxicological hazard, and (4) floodplain importance for desired habitat types and species. We carried out two Monte Carlo (n=15) analyses: one at a 69% CA, the other at 95% CA. Subsequently we ran all four models with the 30 realizations.

The error in the current land cover map gave an uncertainty in water levels of up to 19 cm. Overbank sediment deposition varied up to 100% in the area bordering the main channel, but when aggregated to the whole study area, the variation in sediment trapping efficiency was negligible. The ecotoxicological effects, indicated by the fraction of little owl habitat with a daily cadmium intake exceeding a toxicity

threshold of 148 $\mu\text{g d}^{-1}$, varied between 54 and 60%, aggregated over the distributary. The normalized spread of floodplain importance for species varied between 10 and 15%. Increasing the classification accuracy to 95% significantly lowered the uncertainty of all models applied. Compared to landscaping measures, the effects due to the uncertainty in the land cover map are of the same order of magnitude. Given high financial costs of these landscaping measures, increasing the classification accuracy of land cover maps is a prerequisite for improving the assessment of the efficiency of landscaping measures.

Key words: biodiversity; ecotoxicological hazards; floodplain vegetation; hydrodynamic uncertainty; Monte Carlo analysis; River Rhine; special areas of nature conservation; suspended sediment deposition

1. Introduction

Over the past decades, much effort has been put into the development of models to quantify the impacts of hydrological changes and landscaping measures on flood risk and floodplain ecology. Hydrodynamic models provide estimates of peak water levels and sediment deposition (RWS, 2007; Bates et al., 2010), while ecological models characterize habitat suitability, biodiversity (Lenders et al., 2001; Schipper et al., 2008a) and ecosystem services (Nelson et al., 2009). Such models are routinely used in environmental impact assessments of floodplain restoration projects with landscaping measures that aim to reduce the flood risk and improve the ecological quality of the river area

A land cover map provides essential input for both hydrodynamic and ecological models. In hydrodynamic modeling, land cover maps are commonly used to parameterize floodplain roughness by assigning a roughness coefficient to each land cover type (Chow, 1959). In the context of ecological modeling, land cover maps provide essential information to define and delineate habitat (e.g., Schipper et al. 2008a). Establishing accurate land cover maps of large floodplain areas would require extensive field survey, and therefore remote sensing data are used for this purpose. Over the past decennia, numerous land cover classification schemes have been developed and tested by integrating airborne and satellite imagery, multi-temporal images, different data products (Foody, 2002; Geerling et al., 2007; Antonarakis et al., 2008; Straatsma and Baptist, 2008), or a-priori knowledge (Janssen and Middelkoop,

1992). Typical overall classification accuracies reported in these studies ranged from 70 to 90%.

Several studies have addressed uncertainties in hydrodynamic (Aronica et al., 1998; Pappenberger et al., 2005; Beven, 2006; Apel et al., 2008) and ecological modeling (Elith et al., 2002; Regan et al., 2002; De Nooij et al., 2006). However, the impact of land cover classification errors on hydrodynamic and ecological model output has rarely been quantified. Straatsma and Huthoff (2011) estimated the effect of different error sources in floodplain roughness parameterization on simulated flood water levels. They concluded that land cover classification accuracy (CA) is the dominant error source for distributed floodplain roughness, leading to uncertainties in simulated water levels up to 0.27 m during peak discharges in the Lower Rhine. To our knowledge, effects of land cover CA on other hydrodynamic or ecological models have not yet been quantified.

Our main objective was to assess the uncertainty in hydromorphological and ecological modeling of a lowland river due to classification errors in the land cover map used in an integrated way. Land cover classification error as considered here should be characterized as “ambiguity”, i.e. the degree of confusion among different candidate classes to be assigned to a landscape unit on the map. We quantified this uncertainty with respect to four aspects relevant for hydromorphological and ecological functioning: (1) hydrodynamics, (2) overbank sediment deposition, (3) ecotoxicological hazard, and (4) floodplain importance for desired habitat types and species. Using a suite of quantitative models parameterized for the distributaries of the river Rhine in The Netherlands, we assessed how the model output depended on the classification accuracy of the input land cover maps. Using Monte Carlo re-sampling, we created an ensemble of 15 equally valid land cover maps for the floodplains, based on the CA of 69%, and we generated a second ensemble of 15 maps based on a 95% CA. Subsequently, we ran all four models with the 30 land cover map realizations as input.

2 Study area

In this study, we considered the distributaries of the river Rhine in The Netherlands, excluding the estuary (Fig. 1). At the Dutch-German border, the river Rhine has an average discharge of $2250 \text{ m}^3 \text{ s}^{-1}$, draining a catchment area of $165,000 \text{ km}^2$ (Middelkoop and Van Haselen, 1999). Just downstream of the border, the river Rhine

splits into three main distributaries, i.e., the Waal, the Nederrijn and the IJssel (Fig. 1), which account for approximately two thirds, two ninths and one ninth of the total Rhine discharge, respectively. The three distributaries have an average water gradient of 10 cm per km. The total embanked area amounts to 440 km²; the floodplain area comprises 320 km² out of which 48 km² consists of lakes and side channels. About 62 % of the total embanked area (275 km²) is vegetated. The cross-sectional width between the primary embankments varies between 0.5 and 2.6 km. Design water levels are based on an accepted probability of 1/1250 y⁻¹ of flooding, which is at present associated with a peak discharge of 16,000 m³ s⁻¹ for the Rhine at the German-Dutch border. Currently, the flood protection level of the Rhine branches in the Netherlands corresponds to a discharge of 15,000 m³ s⁻¹. As part of the “Room for the River” project, which is to be finalized by 2015 (RvR, 2011), 24 landscaping measures are implemented along the lower Rhine distributaries to safely convey a discharge of 16,000 m³ s⁻¹. The average suspended sediment deposition on the lower Rhine floodplain amounts to about 0.39 Mton per year, which is an average accumulation rate of 1.72 kg m⁻² y⁻¹ for all river distributaries combined. This equals about 13% of the total suspended sediment load that enters the river system from Germany (Asselman and van Wijngaarden, 2002; Middelkoop et al., 2010). Over the past century, large amounts of sediment-bound trace metals have been deposited on the lowland river Rhine floodplain (Middelkoop, 2000). Through uptake in vegetation and soil-dwelling invertebrates, these metals may enter ecological networks, and potentially induce toxic effects in the organisms exposed. Although the effects of metal exposure are mostly subordinate to influences of other ecosystem stressors, notably flooding (Schipper et al., 2008b; Schipper et al., 2011), toxicological hazards cannot be excluded for certain susceptible species (Van den Brink et al., 2003; Schipper et al., 2008a).

The Dutch parts of the river Rhine are almost entirely protected by the European Union Habitats directive (Council directive 92/43/EEC) and Birds directive (Council directive 79/409/EEC). Each distributary has specific protection goals in terms of carrying capacity for species and habitat types (Alterra, 2012)

3 Materials and methods

Here we describe the primary data that we used, the method for generating alternative land cover maps and the four models we applied in the uncertainty assessment.

3.1 Land cover map

Land cover was based on a map with ecotopes, which are defined as ‘spatial landscape units that are homogeneous as to vegetation structure, succession stage and the main abiotic factors that are relevant to plant growth’ (Van der Molen et al., 2003). This ecotope map provided the land cover used in the models. The map legend is based on the national ecotope system of the Dutch main water bodies (Bergwerff et al., 2003). This system uses a hierarchic structure of ecotopes based on geomorphology and vegetation units, and is further subdivided according to local erosion and deposition rates, inundation frequency and land management. The ecotope map was based on aerial images collected in 2005 (Houkes, 2007). In 2010, a reinterpretation was carried out with respect to brackish environments; we used this reinterpreted version for our study to be up to date. A number of classes needed recoding to match the map purity table. This affected 5% of the area (Supportive information, table 3)

The uncertainty in the ecotope map was determined by Knotters and Brus (2010) based on 406 field observations of 41 terrestrial ecotopes. They computed the map purity, i.e. the percentage of the map area that is correctly classified, and summarized the results in a map purity table. The map purity is based on a statistical model incorporating the spatial variance of the classification errors, see Lohr (1999) for details. The map purity table is similar to the error matrix in classification studies. Knotters and Brus (2010) reported a user’s accuracy of 69% based on eight aggregated ecotope groups. Three problems were noted with the field data collection: (1) The field data comprised point observations, whereas the ecotope map consisted of polygons with an average size of 20700 m². In case of multiple observations per ecotope, variation of vegetation *within* the ecotope could result in multiple, different classifications of a single polygon. This indicates that ecotopes are not fully homogeneous. (2) Ecotopes are determined by inundation frequency, which is hard to discern from plant sociological groups in the field. (3) Time lag between aerial image acquisition and field data collection. Therefore the field data might not be error free, which should be taken into account. Additional quality control is carried out by the river manager, but the increase in CA is not known.

3.2 Ensemble realizations of the ecotope map

Alternative realizations of the ecotope map were generated by conditional simulation as developed by Straatsma and Huthoff (2011). In this conditional simulation, a new ecotope type is assigned to each polygon, conditioned by the classification errors for that ecotope type as presented in the map purity table (Straatsma and Alkema 2009), which is iterated in the supporting information, table 1. We generated 30 alternative realizations of the ecotope map using two classification accuracies at ecotope group level. The first simulation comprised an ensemble of 15 realizations based on the 69% CA assessed by the field validation (Knotters et al., 2008), which underlies the symmetrical map purity table (Straatsma and Alkema, 2009).

Other studies on land cover classification reported accuracies varying between 70% and 92%, depending on the level of detail of the field observations (Van der Sande et al., 2003; Geerling et al., 2007; Straatsma and Baptist, 2008). We therefore chose a 95% CA at ecotope group level to represent an accuracy corresponding with the best methods available. As no map purity table existed with a 95% CA at ecotope group level, we created one based on the 69% CA map purity table. We decreased the off-diagonal values in the map purity table by a factor between 0 and 1. To calibrate this factor, the following steps were undertaken: for each line in the matrix, the difference between the original off-diagonal values and the new values was added to the diagonal value. This led to an increase in the diagonal value and a decrease in the off-diagonal values, leading to a new map purity table with a higher overall CA. The ecotope map purity matrix was subsequently aggregated into eight ecotope groups for which the classification accuracy was computed. The multiplication factor was changed step by step until the CA at ecotope group level reached 95%. The map purity table with a 95% CA at ecotope group level was used to generate the ensemble of 15 alternative ecotope maps with 95% CA (supporting information, table 2).

The conditional simulation was carried out following the method of Straatsma and Huthoff (Straatsma and Huthoff, 2011) and is summarized below. Each line in the map purity table gives the probabilities for alternative classifications of that ecotope type. We computed the cumulative probability by summing up the probabilities along each row in the map purity table. This is illustrated in Fig. 2, which gives the cumulative probabilities for the ecotope type 'High water free natural grassland' (ecotope number 7). For each polygon in the ecotope map, we drew a random number between 0 and 1 from a uniform distribution, and using the cumulative probability we

assigned a new ecotope class to each of the polygons (Fig. 2). In the example, the red arrow represents a random number of 0.71, which would change the polygon from 'High water free natural grassland' to 'Natural levee or floodplain production grassland' (ecotope number 25) for the 69% CA, whereas the polygon would maintain its class at the 95% CA. For each CA, and for each polygon in the original map, this procedure was repeated 15 times, yielding the 69% CA and 95% CA ensembles. Each of the 15 maps in each ensemble can be considered as an equally likely realization of the original, uncertain ecotope map. As the 15 random numbers were drawn once per polygon, i.e. the same numbers were used for both CAs, we ensured that the resulting uncertainty in the modeling only reflected the change in classification accuracy and not a difference due to drawing new random numbers for each of the two ensembles of maps.

3.3 Modeling

We determined the effects of a 69% and a 95% CA on two hydromorphological and two ecological models. Each of the models was run with the 69% CA and 95% CA ensembles of ecotope maps, giving for each CA 15 spatially distributed model outcomes, except for the biodiversity model, which gave spatially aggregated results.

3.3.1 WAQUA hydrodynamic model

The WAQUA model is a two-dimensional hydrodynamic model that numerically solves the Saint Venant equations using a finite difference method (RWS, 2007). It is used by the Dutch Ministry of Infrastructure and Environment for the calculation of water levels and discharge distribution in the complex channel and floodplain areas of the rivers Rhine and Meuse in The Netherlands (RWS, 2007). For the present study, a series of simulations of steady flow in the study area was carried out. The WAQUA model that was used for this study is based on a staggered curvilinear grid. Each of the 886,861 cells represented a column-shaped volume of water with a variable surface area of 700 m² on average. The boundary conditions of the model included the river discharge at the upstream boundary and the water level at the downstream boundary, which was determined using a rating curve. The main spatial model inputs for the WAQUA model were a Digital Terrain Model (DTM), a map with hydraulic structures (e.g. groins, embankments), and a roughness map. Roughness maps were based on the ecotope map using the Baseline database and software (Hartman and

Van den Braak, 2007). The Baseline software reclassifies each ecotope class to a roughness class (Table 1) using a lookup table, and assigns vegetation structural characteristics. Stage dependent roughness is computed at run time by applying the roughness model of Klopstra et al. (1997)

We used WAQUA with the 69% and 95% CA ensembles as input, giving 30 model parameterizations, which were subsequently run at nine stationary discharges (3,500 - 4,000 - 5,000 - 6,000 - 7,000 - 8,000 - 10,000 - 12,000 and 16,000 m³ s⁻¹) at the upstream boundary at Emmerich, Germany. At the lowest simulated discharge of 3,500 m³ s⁻¹, the low-lying floodplains are just inundated. The highest discharge corresponds to the current design discharge with a statistical return period of 1,250 years. The simulation time for the runs was set to three days to stabilize the water levels and discharge distribution. Output of the computations consisted of spatially distributed values of the Chézy C roughness coefficient, flow velocities, water levels, and the discharge distribution over the bifurcation points.

3.3.2 SEDIFLUX model for suspended sediment deposition

We used the GIS-embedded SEDIFLUX model to calculate the transport and deposition of suspended sediment, using the 2D water flow patterns calculated by the WAQUA model. This model was developed and tested for floodplain sections along the river Rhine by Middelkoop and Van der Perk (1998). For this study we used a similar approach as followed by Straatsma et al. (2009) to estimate the average deposition rate. For each of the nine discharge levels, the suspended sediment concentration at the upper model boundary was established using a sediment rating curve derived for the 1970-2006 observation record at the German-Dutch border. The main output of the SEDIFLUX-model includes the 2D pattern of sediment deposition rate (kg m⁻² d⁻¹) for each discharge level. The average annual deposition (kg m⁻² y⁻¹) was subsequently calculated by summing the products of these calculated sediment deposition rates for each discharge level and the average annual number of days that the corresponding discharge classes occurred in the 1970-2006 period. The output consisted of the spatial pattern in the spread of the annual average sediment deposition for two classification accuracies.

3.3.4. Ecotoxicological hazards

Ecotoxicological hazards due to sediment contamination were assessed for the little

owl (*Athene noctua*), which is one of the species potentially affected by trace metals in the lowland river Rhine floodplain (Van den Brink et al., 2003; Schipper et al., 2008a). We defined a simplified food web with three levels: (1) vegetation, beetles, earthworms and wild berries, (2) common vole, bank vole, common shrew, and wood mouse, and (3) the little owl at the top level (Schipper et al. 2012). Ecotoxicological hazards were assessed for those ecotopes providing suitable habitat to the little owl and were based on the daily intake of cadmium through contaminated food:

$$DI = DFI \cdot \sum_{i=1}^{n_j} f_{i,j} \cdot C_i \quad (1)$$

where DI = daily intake of cadmium ($\mu\text{g d}^{-1}$), DFI = daily food intake (80 g d^{-1} ; (Schönn et al., 2011), f_i = weight fraction of prey type i in the little owl's diet in ecotope j (dimensionless), n_j = number of prey types in ecotope j , C_i = cadmium concentration of prey type i ($\mu\text{g g}^{-1}$). Dietary fractions $f_{i,j}$ were calculated by adjusting initial diet fractions derived from the literature (Supportive information, table 4) according to the habitat suitability of the ecotope type for the respective prey items. Corrected fractions were rescaled to ensure that they summed to 1:

$$f_{i,j} = \frac{f_{i,i} \cdot HS_{i,j}}{\sum_{i=1}^m f_{i,i} \cdot HS_{i,j}} \quad (2)$$

where $f_{i,i}$ = initial fraction (weight-based, dimensionless) of prey type i in the little owl's diet, and $HS_{i,j}$ = habitat suitability of ecotope type j for prey type i , expressed as a dimensionless value between 0 and 1. Habitat suitability was calculated based on ecotope suitability ($ES_{i,j}$; Supportive information, table 5) as described in Schipper et al. (2008a). Irrespective of habitat suitability, small mammals were absent from areas beyond their maximum colonization distance from flood-free areas (Schipper et al. 2008a), which were defined as locations where the ground surface elevation is higher than the water level resulting from a discharge that is exceeded 2 days per year ($7200 \text{ m}^3 \text{ s}^{-1}$ at Emmerich). Cadmium concentrations C_i in small mammal prey were calculated based on their assimilation of cadmium from contaminated first level food web items, whereas cadmium concentrations C_i in first-level items were derived from soil concentrations with regression equations or bioaccumulation factors (Schipper et al. 2008a). Soil cadmium concentrations were derived from a soil quality map of the three river distributaries, scale 1:25000 (Hin et al., 2001), representing contaminant concentrations in the upper 50 cm of the soil profile. This polygon map consisted of

seven classes with cadmium concentrations of 0, 1, 2, 3, 4, 6, and 10 mg kg⁻¹ dry weight.

The daily intake calculations were performed at a 10x10 m spatial resolution. To obtain an indication of toxic effects, daily intake values were compared with a toxicity threshold of 148 µg cadmium per day (Schipper et al., 2012) Results were summarized as the fraction of habitat (i.e., $HS_{\text{little owl}} > 0$) with a cadmium DI > 148 µg d⁻¹. In addition, the results were summarized per river branch by computing the map fraction as a function of the number of realizations that exceeded the toxicity threshold. For example, 5% of the river IJssel showed seven runs higher than the toxicity level. The toxicity consistency was subsequently computed as the map fraction that was always above, or always below (n=15, or n=0) the toxicity level.

3.3.5. BIO-SAFE model for biodiversity potential

BIO-SAFE is a model for quantification of (potential) values of riverine landscapes for protected and endangered species, depending on ecotope distribution (potential habitat) and ecological and legal status of species and habitat types. De Nooij et al. (2006) and Lenders et al. (2001) described the indices used for quantification of (potential) values of riverine landscapes and the setup, validation and sensitivity analysis of BIO-SAFE. The model was developed for the floodplains of the rivers Rhine and Meuse in the Netherlands, Germany, France, Belgium (De Nooij et al., 2004) and the river Vistula in Poland (Wozniak et al., 2009). For the present study we included the specified protection goals in terms of carrying capacity for species and habitat types for each distributary, according to European legislation for protection of nature areas (Habitats and Birds Directive). For each species and habitat type, the Floodplain Importance score (FI) was computed. High FI scores represent a high (potential) value of an area for a particular species or habitat type.

4 Results

The effects of the uncertainties in the land cover maps on the four models are presented in this section. The spatial patterns in the uncertainties in hydrodynamics, sediment deposition and ecotoxicological hazards are presented in maps (Fig. 3, 4). Results are described by the 68% confidence interval for selected model outcomes ($P_{84} - P_{16}$), equaling the interval between one standard deviation above and below the mean in case of a normal distribution. We will refer to this statistic as the *spread*.

Summary statistics were calculated per classification accuracy for the three distributaries (Table 2). Details on the model outcomes are given in subsequent sections.

4.1 Uncertainty in hydrodynamics

The spread in water levels occurring at the $16,000 \text{ m}^3\text{s}^{-1}$ design discharge varied spatially (Fig. 3a-b, 4a-b). A small spread was found for the upstream part of the Waal; short sections in the IJssel showed the largest spread. The effect of increased CA becomes apparent when comparing part a and b of figures 3 and 4: at a 69% CA, the river IJssel showed a spread of up to 19 cm at the design discharge, which was reduced to 7 cm at a 95% CA. The Waal (Fig. 4) has a lower fractional discharge over the floodplain area than the IJssel, which resulted in a 12 cm spread from a 69% CA at the design discharge. Still, an increased CA reduced the maximum spread for the Waal to 5 cm (Table 2). The results for the Nederrijn fall in between those obtained for the Waal and IJssel. In general, the spread was reduced by approximately 60%, depending on the distributary (Table 2). Note that the spread filters out the extremes in the variation that was found. The maximum difference in water levels that we found was 44 cm in the IJssel. To summarize the spread in the three distributaries at different discharge levels, we computed the spread at the river axes at each river kilometer for each of the nine stationary discharges (Fig. 5). The spread in water level shows a strong linear correlation with the discharge ($r = 0.96 - 0.99$ for the maximum spread per river branch; $r = 0.96 - 0.98$ for the median spread per river branch).

The variation in roughness also affected the discharge distribution. Lower roughness on a particular side of the bifurcation point for a specific realization of the ecotope map led to a lower water level at that side. This increased the discharge into that branch. As a result of this effect, the spread in discharge ranged between 65 and $89 \text{ m}^3\text{s}^{-1}$ for the 69% CA ensemble, and between 37 and $58 \text{ m}^3\text{s}^{-1}$ for a 95% CA (Table 2) at design discharge. These discharge variations lead to differences in water level of 3, 7, and 7 cm for the river Waal, Nederrijn, and Lek, respectively (Fig. 7 in Straatsma and Huthoff (2010)).

4.2 Uncertainty in sediment deposition

The annual average suspended sediment deposition (Fig. 3c, 4c) is largest in the area between the main channel and the minor embankments. Here, the inundation

frequency is high; during inundation, the flow velocity decreases and sediment settles. Comparing the spatially distributed annual sedimentation and spread (Fig. 3, 4 c-e), we found that: (1) the river IJssel has a lower median sediment deposition rate than the River Waal, (2) the spread in the annual deposition is lower in IJssel River than the River Waal, (3) the spread in the deposition is an order of magnitude lower than the median of the deposition, (4) the spatial distribution of the spread is highly variable. The results for the Nederrijn again take the intermediate position with respect to deposition rate. The pattern of high deposition close to the main channel is similar to the other two river branches. To get insight in the uncertainty relative to the total deposition, we normalized the spread (NS; Normalized Spread) by dividing the spread map by the median map. NS map was summarized by a histogram (Fig. 6) for each of the three distributaries. All show a similar distribution of the NS: 70% of the map has a NS of less than 0.2 at a 69% CA, which increases to 90-95% of the map for a 95% CA.

Table 3 shows the distribution statistics (spread) of the annual sediment deposition aggregated for each river branch and the entire model area. The uncertainty at the scale of the river branches is very small (spread \ll 1% of the median value for both 69% CA and 95% CA). The 5000 m³s⁻¹ discharge class contributes most (20%) to the total sediment deposition on the Rhine floodplains. However, the 7000 m³s⁻¹ discharge class contributes most to the uncertainty of the average annual sediment deposition, except for the IJssel distributary where the 5000 m³ s⁻¹ discharge class contributes most to the uncertainty. This is likely due to the fact that the low-lying IJssel floodplains are inundated during lower discharges than the floodplains along the other distributaries.

With a 95% CA, there was slightly less overbank deposition in the Waal and Nederrijn distributaries, which was compensated for by slightly larger deposition along the Bovenrijn and IJssel distributaries. This is likely due to the fact that in the conditional simulation procedure, the probability of assigning an ecotope with a higher roughness is greater than assigning an ecotope with a lower roughness (Straatsma and Huthoff, 2011). In general, this causes larger sedimentation rates close to the river channel and concurrently smaller sedimentation rates further away from the river in the 69% CA scenario than in the 95% CA scenario.

4.3 Uncertainty in ecotoxicological hazards

For the 69% CA, the spread in ecotoxicological hazards (i.e., the spread in the fraction of little owl habitat with a daily cadmium intake exceeding the corresponding toxicity threshold) ranged from 0.03 for the Nederrijn and Waal to 0.06 for the IJssel (Table 2; Fig. 3f, 4f). The spread was somewhat lower for the 95% CA (Table 2). On average, toxicological hazards were largest for the IJssel and smallest for the Nederrijn. This reflects differences in the average soil cadmium concentrations, which are 2.85 and 1.36, and 3.05 mg kg⁻¹ for the Waal, Nederrijn and IJssel, respectively. The number of times a polygon exceeded the threshold showed a stronger bimodal pattern for the 95% CA than for the 69% CA, as illustrated by the increase in areas that never (0) or in all cases (15) exceeded the threshold (Fig.3; Fig. 4). The histogram of exceedance values per river branch (Fig. 7) showed the same pattern. The consistency of the output, defined as the habitat area on the map that either always or never exceeded the threshold for all 15 model runs, increased from a map fraction of 0.52 to 0.87 (Table 2) for the IJssel. The other distributaries showed a smaller increase.

Surprisingly, we found little differences in the total map fraction with unsuitable habitat within an ensemble (Table 2). For the Bovenrijn-Waal the fraction of unsuitable habitat ranged between 0.39 and 0.42, for the Pannerdensch Kanaal-Nederrijn-Lek between 0.16, and 0.19. However, the fractions of unsuitable habitat were much larger for the 95% CA ensemble than for the 69% ensemble. Soil cadmium concentrations were on average slightly higher for ecotope types providing little owl habitat (i.e., grassland ecotopes) than for ecotope types that may be confused with grassland. Hence, confusion of grassland with these other ecotope types resulted in a decrease in the average soil cadmium concentration within the little owl habitat. As the probability for confusion with other types was higher for the 69% CA ensemble, the fraction of habitat with daily intake values below the toxicity threshold was lower for the 69% CA ensemble.

4.4 Uncertainty in biodiversity values

The potential biodiversity values of the floodplains (FI scores) differed remarkably between habitat types and species protected by the EU legislation (Natura 2000 sites) within each river branch (Figures 8, 9). The spreads were systematically larger for the 69% CA ensemble. Absolute values of the FI scores were higher for the 69% CA ensemble for all habitat types, except for “Xeric sand calcareous grasslands” and

“Softwood alluvial forest with white willow” (H6120 and H91E0_A) in the Nederrijn, “Xeric sand calcareous grasslands” (H6120) in the IJssel, and “lowland hay meadow with meadow foxtail” (H6510_B) in the Waal (Figure 8; Table 4). The FI score of the 95% CA ensemble was even 5.8 times higher for “Hydrophilous tall herb fringe communities of plains along dry forests” for all Rhine branches combined. The higher FI scores for the 69% ensemble was caused by the map purity table, which converted meadows more often to herbeceous vegetation, than the other way around, leading to a systematic difference in the ecotope distribution.

These general patterns also held for the protected species (Figure 9). The 69% CA resulted in higher FI scores for all species, except Greylag Goose, Eurasian Curlew, Greater White-fronted Goose (*Anser anser*, *Numenius arquata*, and *Anser albifrons*), and wider confidence intervals, except for Northern Shoveler (*Anas clypeata*). However, FI scores and confidence intervals increased less for species than for habitat types. The scale of application of the BIO-SAFE model also influenced the results. The uncertainty is larger for separate river branches than for the application of BIO-SAFE to the whole study area, which is visible in the spreads (Figure 9 top panel versus other panels).

5 Discussion

Uncertainty in hydrodynamic and ecological models has many sources (Regan et al., 2002; Walker et al., 2003). Ideally, all would be combined in a single study to find the overall error. In this study, we quantified the effects of land cover classification error on hydrodynamic and ecological model output. We focused on water levels, suspended sediment deposition, ecotoxicological hazards and floodplain importance for different habitat types and species. The CA of the land cover map was determined from field data (Knotters et al., 2008). In this study, large effects were found of land cover CA on hydromorphological and ecological modeling. This uncertainty points to the need for an unambiguous quality assessment of the ecotope map. Below, we will first discuss model output before we put our results in perspective by comparing them to other factors that influence hydrodynamics and ecology: (1) landscaping measures in the context of the “Room for the River” project, (2) scenario studies that provide insight in a possible situation in 2050, and (3) uncertainty due to vegetation succession.

5.1 Hydrodynamic and ecological model output

The reference hydrodynamic model used in this study was calibrated on historic flood events. Strictly speaking, each new realization of the ecotope map would require a re-calibration of the hydrodynamic model such that each realization accurately reproduces the historic flood events. In this study, the re-calibration step has been omitted, due to the large efforts involved in calibration of a 2D model with two bifurcation points. Calibration of a hydrodynamic model would normally reduce the prediction error by comparing model output with measured discharges, or water levels. Including the additional calibration step is part of a follow up study currently carried out. Calibration of the sedimentation model is more labor intensive as deposition rates need to be measured by placing sediment traps in the floodplain (Middelkoop and Asselman, 1998; Thonon, 2006). Still, further calibration of SEDIFLUX for larger areas and for different flood magnitudes could reduce the overall prediction error of spatially distributed sedimentation rates. With the spread maps presented here one can target the most sensitive areas for placing the sediment traps. Currently, no data are available for calibrating and validating the output of the ecotoxicological model and BIOSAFE, and hence the errors in the land cover map directly influence the output.

Increasing the CA from 69% to 95% led to a 60% reduction in the uncertainty in flood water levels, a 50% increase in the map fraction that has a normalized spread of 0.2 or less for suspended sediment deposition, and a 6-67% increase in the consistency of the ecotoxicological hazard assessment for the Little Owl. Using the type of Monte-Carlo tests carried out in this study, it is possible to determine the required classification accuracy based on the accepted level of uncertainty in the model output. For example, if the uncertainty in the water levels should be no larger than a spread of 10 cm, the required CA of the ecotope map would be 77%, 86%, and 89% for the rivers Waal, Nederrijn, and IJssel, respectively assuming a linear relationship between CA and uncertainty in output for the sake of this example. Similarly, if benchmarks were set for the required accuracy in suspended sediment deposition modeling, ecotoxicological hazard modeling, or floodplain biodiversity modeling, the corresponding CA could be established. However, at the moment no such benchmarks exist, not even for water level, which represents the key factor for flood hazard assessments. Establishing such benchmarks is a societal and political choice; how much risk are we prepared to take? The answer would influence the

amount of data to be collected, the methods to be developed by the remote sensing community, and the models applied in flood hazard assessment. In the meantime, scientists could further study the relationship between CA and uncertainty to address the assumption of a linear relationship.

5.2 Other sources of uncertainty in hydrodynamic and ecological model output

The “Room for the River” landscaping measures (Fig. 1) should facilitate an increase in discharge capacity from 15,000 to 16,000 m³s⁻¹ by the year 2015. Various measures are carried out to increase the cross-sectional area of the high-water bed of the river, between the primary river dikes, including the creation of side channels, dike relocation, and floodplain lowering. The ecotope distribution will also be changed, primarily due to targeted ecological restoration. The required flood level reduction is 20 cm for the Waal, 30 cm for the Nederrijn, and 40 cm for the IJssel (Deltares, 2011; RvR, 2011). The spread in the water levels for a 69% CA was 12, 15, and 19 cm for the Waal, Nederrijn and IJssel, respectively (Table 3), corresponding with approximately 50% of the reduction in the water levels required according to “Room for the River.” Given the societal significance of flooding and the high cost of the landscaping measures, i.e. €2.3 billion (Waterforum, 2011), the higher 95% CA in the underlying land cover maps is indispensable. This would reduce the spread to 5, 7, and 7 cm for Waal, Nederrijn and IJssel, respectively, which is around 20% of the task in the “Room for the River”. The landscaping measures presently undertaken in the Room for the River project will locally dramatically enhance overbank sedimentation rates, up to a factor 5 to 10 (Asselman, 1999; Thonon et al., 2007). Still, the areal extent of the measures is too small to result in significant changes in total sediment trapping by the embanked floodplains.

Scenario studies are commonly used to explore the effects of future conditions on the fluvial area. Recently, a scenario study was carried out by Straatsma et al. (2009) to explore options for accommodating a design discharge of 17,000 m³s⁻¹ at Emmerich in 2050. They studied only the river Waal, and their ‘best’ scenario with respect to flood hazard reduction yielded an average lowering of the water level of 65 cm, which was 5 cm less than required. As the uncertainty due to land cover classification error at a 69% CA is 12 cm for the Waal, the uncertainty due to classification errors is less relevant for the 2050 temporal horizon. Similarly, the sediment deposition, and ecotoxicological hazard are influenced more by the

projected landscaping measures in 2050 than by CA error. Potential biodiversity values are the exception; the CA presents an equal variation in BIO-SAFE output as the effects of landscaping measures up to 2050.

Vegetation succession is another source of changes in ecotopes. As changes in vegetation due to succession are expected to be small within the 6-year mapping interval of the ecotope map, we did not consider succession. However, the target vegetation that may develop under the 'Room for the River' plans will eventually lead to a higher – but yet harder to predict – hydraulic roughness, and thus an increase in water levels (Makaske et al., (2011)). Since more natural vegetation is likely to be patchier than the present-day vegetation that still strongly reflects the cultivation of the floodplain, the classification accuracy of vegetation maps will be an increasingly challenging task.

Conclusions

We assessed the effects of land cover classification errors on hydrodynamic and ecological model output for the three distributaries of the river Rhine in the Netherlands. Model output pertained to water levels and discharge distribution during design discharge, annual average suspended sediment deposition, ecotoxicological hazard for the little owl, and biodiversity values. Based on a conditional simulation of ecotope maps, we created two ensembles of 15 maps each, one based on a 69% classification accuracy (CA), and one with a 95% CA. We conclude that:

- A 69% CA gave a 12 to 19 cm uncertainty in the water levels during design discharge, which is approximately 50% of the task set for the proposed flood mitigation measures for 2015. An increased CA of 95% leads to a relevant improvement.
- Ambiguities in the land cover map led to uncertainty in the discharge distribution over the bifurcation points. Increasing the CA from 69 to 95% reduces the uncertainty by almost 50%. River management should therefore advocate the reduction of classification errors in land cover maps.
- The spread in the sediment deposition rate was spatially highly variable and depended strongly on the CA. An increase of the CA reduced uncertainty in sediment deposition significantly. This is important for the design of local landscaping measures and the expected morphological changes. For the distributaries as a whole, the deposition showed negligible variation. For

assessing the sediment trapping efficiency at the scale of an entire delta, increasing the land cover CA is therefore not relevant.

- Based on the ecotoxicological modeling, the map fraction with unsuitable habitat did not depend strongly on the CA for ensemble averages over the distributaries. However, the consistency of the ensemble output increased with a higher CA. This implies that targeting ecological restoration to specific species as the Little Owl will be more accurate and efficient when an unambiguous land cover map.
- For potential biodiversity values, BIO-SAFE predicted on average higher Floodplain Importance scores for a lower CA, due to the larger deviation from the current map. Therefore, the current map might underestimate the potential biodiversity of the Rhine branches. A high CA would justify ecological rehabilitation works better, because the current situation is known better and the target can be specified more clearly.
- Investments in higher classification accuracy seem reasonable given the large investments that are needed to carry out the mitigating measures. For scenario studies with a long temporal horizon, uncertainty in land cover classification is less relevant.

Given the future challenges for river and floodplain management, such as climate change, nature restoration, and housing demands, uncertainty reduction in land cover mapping will pay off as large amounts of money are involved in projects worldwide. Using an integrated approach as presented in this paper, benchmarks may be established, which is a political choice on the risk we want to take with respect to flood hazard and river health. A high map accuracy will give the river manager a better argument for landscaping measures, modelers a higher quality output, remote sensing community a tangible targets for land cover CA, and the public a safer and more healthy river.

Acknowledgements

This research was partly supported by the NWO-LOICZ program under contract number 01427004, and the FloodControl2015 program (www.floodcontrol2015.com). Funding for A. Schipper was provided by the European Commission under the Seventh Framework Program on Environment (ENV.2007.3.3.1.1: CADASTER: In-

silico techniques for hazard, safety, and environmental risk assessment - grant agreement number 212668).

References

- Alterra, 2012. Natura 2000.
<http://www.synbiosys.alterra.nl/natura2000/gebiedendatabase.aspx?subj=n2k>,
date accessed 19-01-2012.
- Antonarakis, A.S., Richards, K.S., Brasington, J., 2008. Object-based land cover classification using airborne LiDAR. *Remote Sensing of Environment* 112, 2988 - 2998.
- Apel, H., Merz, B., Thielen, A.H., 2008. Quantification of uncertainties in flood risk assessments. *International Journal of River Basin Management* 6, 149 - 162.
- Aronica, G., Hankin, B., Beven, K., 1998. Uncertainty and equifinality in calibrating distributed roughness coefficients in a flood propagation model with limited data. *Advances in Water Resources* 22, 349-365.
- Asselman, N.E.M., 1999. The use of floodplain sedimentation measurements to evaluate the effects of river restoration works. Geological Society, London, Special Publications 1999 163, 111-122.
- Asselman, N.E.M., van Wijngaarden, M., 2002. Development and application of a 1D floodplain sedimentation model for the River Rhine in The Netherlands. *Journal of Hydrology* 268, 127-142.
- Bates, P.D., Horritt, M.S., Fewtrell, T.J., 2010. A simple inertial formulation of the shallow water equations for efficient two-dimensional flood inundation modelling. *Journal of Hydrology* 387, 33-45.
- Bergwerff, J., Knotters, A., Vreeken, M., Willems, D., 2003. Methodeherziening ecotopenkartering (in Dutch). RWS-AGI, Delft, report nr. AGI-GEA-2003.
- Beven, K., 2006. A manifesto for the equifinality thesis. *Journal of Hydrology* 320, 18-36.
- Chow, V.T., 1959. Open channel hydraulics. McGraw Hill, New York.
- De Nooij, R.J.W., Lenders, H.J.R., Leuven, R.S.E.W., De Blust, G., Geilen, N., Goldschmidt, B., Muller, S., Poudevigne, I., Nienhuis, P.H., 2004. BIO-SAFE: assessing the impacts of physical reconstruction on protected and endangered species. *River Research and Applications* 20, 299-313.
- De Nooij, R.J.W., Lotterman, K.M., van de Sande, P.H.J., Pelsma, T., Leuven, R.S.E.W., Lenders, H.J.R., 2006. Validity and sensitivity of a model for assessment of impacts of river floodplain reconstruction on protected and endangered species. *Environmental Impact Assessment Review* 26, 677-695.
- Deltares, 2011. Planning kit educational version.
<http://www.wldelft.nl/soft/blokkendoos/index.html>, accessed 21-6-2011, date accessed
- Elith, J., Burgman, M.A., Regan, H.M., 2002. Mapping epistemic uncertainties and vague concepts in predictions of species distribution. *Ecological Modelling* 157, 313-329.
- Foody, G.M., 2002. Status of land cover classification accuracy assessment. *Remote Sensing of Environment* 80, 185-201.
- Geerling, G.W., Labrador-Garcia, M., Clevers, J., Ragas, A., Smits, A.J.M., 2007. Classification of floodplain vegetation by data-fusion of Spectral (CASI) and LiDAR data. *International Journal of Remote Sensing* 28, 4263 – 4284.

- Hartman, M.R., Van den Braak, W.E.W., 2007. Baseline manual, baseline 4.03. RIZA, Arnhem, report nr. RIZA-werkdocument 2004-170X, pp. 128.
- Hin, J., Van de Laar, E., Menke, U., 2001. Definitiestudie bodemkwaliteitskaarten Rijntakken (Definition study soil quality map). RIZA, Arnhem, report nr. RIZA report 2001.054, pp. 92.
- Houkes, G., 2007. Ecotopenkartering Rijntakken-Oost 2005: Biologische monitoring zoete rijkswateren (in Dutch). RWS-AGI, Delft, report nr. pp. 40.
- Janssen, L.L.F., Middelkoop, H., 1992. Knowledge-based crop classification of a landsat thematic mapper image. *International Journal of Remote Sensing* 13, 2827-2837.
- Klopstra, D., Barneveld, H., Van Noordwijk, J.M., Van Velzen, E.H., 1997. Analytical model for hydraulic roughness of submerged vegetation. 27th international IAHR conference San Francisco, pp. 775-780.
- Knotters, M., Brus, D.J., 2010. Sampling for validation of ecotope maps of floodplains in the Netherlands: a model-based versus a design-based approach. *Proceedings of the Ninth International Symposium on Spatial Accuracy Assessment in Natural Resources and Environmental Sciences*, Leicester, UK, p. 3.
- Knotters, M., Brus, D.J., Heidema, A.H., 2008. Validatie van de ecotopenkaarten van de rijkswateren. Alterra, Wageningen, report nr. Alterra-rapport 1656, pp. 47.
- Lenders, H.J.R., Leuven, R.S.E.W., Nienhuis, P.H., De Nooij, R.J.W., Rooij, V., 2001. BIO-SAFE: a method for evaluation of biodiversity values on the basis of political and legal criteria. *Landscape and Urban Planning* 55, 121-137.
- Lohr, S.L., 1999. *Sampling: design and analysis*. Duxbury press, Pacific Grove, USA.
- Makaske, B., G.J., M., N.G., V.d.B., H.P., W., 2011. The influence of floodplain vegetation succession on hydraulic roughness: is ecosystem rehabilitation in Dutch embanked floodplains compatible with flood safety standards? *Ambio* 40, 370-376.
- Middelkoop, H., Asselman, N.E.M., 1998. Spatial variability of floodplain sedimentation at the event scale in the Rhine-Meuse delta, The Netherlands. *Earth Surface Processes and Landforms* 23, 561-573.
- Middelkoop, H., Erkens, G., Van der Perk, M., 2010. The Rhine delta—a record of sediment trapping over time scales from millennia to decades. *Journal of Soils and Sediments* 10, 628-639.
- Middelkoop, H., Van der Perk, M., 1998. Modelling spatial patterns of overbank sedimentation on embanked floodplains. *Geografiska Annaler* 80 A, 95-109.
- Middelkoop, H., Van Haselen, C.O.G., 1999. Twice a river: Rhine and Meuse in the Netherlands. RIZA, Arnhem, report nr. 99.003.
- Nelson, E., Mendoza, G., Regetz, J., Polasky, S., Tallis, H., Cameron, D., Chan, K.M., Daily, G.C., Goldstein, J., Kareiva, P.M., Lonsdorf, E., Naidoo, R., Ricketts, T.H., Shaw, M., 2009. Modeling multiple ecosystem services, biodiversity conservation, commodity production, and tradeoffs at landscape scales. *Frontiers in Ecology and the Environment* 7, 4-11.
- Pappenberger, F., Beven, K., Hunter, N.M., Bates, P., Gouweleeuw, B.T., Thielen, J., De Roo, A.P.J., 2005. Cascading model uncertainty from medium range weather forecasts (10 days) to rainfall-runoff models to flood inundation predictions within the European Flood Forecasting System (EFFS). *Hydrology and Earth System Sciences* 9, 381-393.

- Regan, H.M., Colyvan, M., Burgman, M.A., 2002. A taxonomy and treatment of uncertainty for ecology and conservation biology. *Ecological Applications* 12, 618-628.
- RvR, 2011. Room for the river: a safer and more attractive rivers region. <http://www.ruimtevoorderivier.nl/meta-navigatie/english>, date accessed 08-06-2011.
- RWS, 2007. Users guide WAQUA: Technical Report SIMONA 92-10. <http://www.waqua.nl/systeem/documentatie/usedoc/slib3d/ug-slib3d.pdf>, date accessed 13-02-2008.
- Schipper, A.M., Loos, M., Ragas, A.M.J., Lopes, J.P.C., Nolte, B., Wijnhoven, S., Leuven, R.S.E.W., 2008a. Modeling the influence of environmental heterogeneity on heavy metal exposure concentrations for terrestrial vertebrates in river floodplains. *Environmental Toxicology and Chemistry* 27, 919-932.
- Schipper, A.M., Lotterman, K., Leuven, R.S.E.W., Ragas, A.M.J., De Kroon, H., Hendriks, A.J., 2011. Plant communities in relation to flooding and soil contamination in a lowland Rhine River floodplain. *Environmental Pollution* 159, 182-189.
- Schipper, A.M., Wijnhoven, S., Baveco, H., Van den Brink, N.W., 2012. Contaminant exposure in relation to spatio-temporal variation in diet composition: A case study of the little owl (*Athene noctua*). *Environmental Pollution* 163, 109-116.
- Schipper, A.M., Wijnhoven, S., Leuven, R.S.E.W., Ragas, A.M.J., Hendriks, J.A., 2008b. Spatial distribution and internal metal concentrations of terrestrial arthropods in a moderately contaminated lowland floodplain along the Rhine River. *Environmental Pollution* 151, 17-26.
- Schönn, S., Scherzinger, W., Exo, K.-M., Ille, R., 2011. *Der Steinkauz*. Ziemsen Verlag, Wittenberg.
- Straatsma, M., Huthoff, F., 2011. Uncertainty in 2D hydrodynamic models from errors in roughness parameterization based on aerial images. *Physics and Chemistry of the Earth, Parts A/B/C* 36, 324-334.
- Straatsma, M., Schipper, A., van der Perk, M., van den Brink, C., Leuven, R., Middelkoop, H., 2009. Impact of value-driven scenarios on the geomorphology and ecology of lower Rhine floodplains under a changing climate. *Landscape and Urban Planning* 92, 160-174.
- Straatsma, M.W., Alkema, D., 2009. Error propagation in hydrodynamics of lowland rivers due to uncertainty in vegetation roughness parameterization FloodControl2015, report nr. 2009-06-05, pp. 44.
- Straatsma, M.W., Baptist, M.J., 2008. Floodplain roughness parameterization using airborne laser scanning and spectral remote sensing. *Remote Sensing of Environment* 112, 1062-1080.
- Straatsma, M.W., Huthoff, F., 2010. Relation between accuracy of floodplain roughness parameterization and uncertainty in 2D hydrodynamic models. Faculty of ITC, University of Twente, Enschede, report nr. pp. 49.
- Thonon, I., 2006. Deposition of sediment and associated heavy metals on floodplains. *Physical Geography*. Utrecht University, Utrecht, p. 174.
- Thonon, I., H., M., Van der Perk, 2007. The influence of floodplain morphology and river works on spatial patterns of overbank deposition. *Netherlands Journal of Geosciences — Geologie en Mijnbouw* 86, 63-76.

- Van den Brink, N.W., Groen, N.M., De Jonge, J., Bosveld, A.T.C., 2003. Ecotoxicological suitability of floodplain habitats in The Netherlands for the little owl (*Athene noctua vidalli*). *Environmental Pollution* 122, 127-134.
- Van der Molen, D.T., Geilen, N., Backx, J.J.G.M., Jansen, B.J.M., Wolfert, H.P., 2003. Water Ecotope Classification for integrated water management in the Netherlands. *European Water Management Online*.
http://www.ewaonline.de/journal/2003_03.pdf, date accessed 16-06-2011.
- Van der Sande, C.J., De Jong, S.M., De Roo, A.P.J., 2003. A segmentation and classification approach of IKONOS-2 imagery for land cover mapping to assist flood risk and flood damage assessment. *International Journal of Applied Earth Observation and Geoinformation* 4, 217-229.
- Walker, W.E., Harremoes, P., Rotmans, J., Van der Sluijs, J.P., Van Asselt, M.B.A., Janssen, P., Krayner von Kraus, M.P., 2003. Defining Uncertainty A Conceptual Basis for Uncertainty Management in Model-Based Decision Support. *Integrated Assessment* 4, 5-17.
- Waterforum, 2011. Budgetruimte voor de rivier blijft op 2.3 miljard euro.
<http://www.waterforum.net/nieuws/1544-budget-ruimte-voor-de-rivier-blijft-op-23-miljard-euro>, date accessed 21-6-2011.
- Wozniak, M., Leuven, R.S.E.W., Lenders, H.J.R., Chmielewski, T.J., Geerling, G.W., Smits, A.J.M., 2009. Assessing landscape change and biodiversity values of the Middle Vistula river valley, Poland, using BIO-SAFE. *Landscape and Urban Planning* 72, 210-219.

Table 1 Ecotope codes, descriptions and associated roughness classes.

	Ecotope code	Ecotope description	Roughness class
1	H-REST	High water free temporarily bare	Rest
2	HA-1	High water free agriculture	Agricultural land
3	HA-2	High water free built-up area	Paved / Built-up area
4	HB-1	High water free natural forest	Natural forest
5	HB-2	High water free shrubs	Shrubs
6	HB-3	High water free production forest	Production forest
7	HG-1	High water free natural grassland	Natural meadows
8	HG-1-2	High water free grassland (natural or production)	Production / natural meadows
9	HG-2	High water free production grassland	Production meadows
10	HM-1	High water free reeds	Reeds and other helophytes
11	HR-1	High water free herbaceous vegetation	Herbaceous vegetation
12	I.1	High water free temporarily bare	Rest
13	II.2	Sweet sand bars	Bare river bar
14	III.2-3	Low dynamic hard substrate influenced by sweet to brackish water	Paved / Builtup area
15	IV.8-9	Species poor helophytes swamp/Species rich reed swamp	Reeds and other helophytes
16	IX.a	Agriculture on the shoreline	Agricultural land
17	O-U-REST	Natural levee or floodplain temporarily bare	Rest
18	O-UA-1	Natural levee or floodplain agriculture	Agricultural land
19	O-UA-2	Natural levee or floodplain builtup area	Paved / Builtup area
20	O-UB-1	Natural levee or floodplain forest	Natural forest
21	O-UB-2	Natural levee or floodplain shrubs	Shrubs
22	O-UB-3	Natural levee or floodplain production forest	Production forest
23	O-UG-1	Natural levee or floodplain grass land	Natural grassland
24	O-UG-1-2	Natural levee or floodplain grass land (natural or production)	Production / natural meadows
25	O-UG-2	Natural levee or floodplain production grassland	Production meadows
26	O-UK-1	Natural levee or floodplain unvegetated	Rest
27	O-UR-1	Natural levee or floodplain herbaceous vegetation	Herbaceous vegetation
28	OK-1	Unvegetated natural levee	Rest
29	R	Temporarily bare	Rest
30	REST	Temporarily bare	Rest
31	U-REST	Floodplain temporarily bare	Rest
32	UA-1	Floodplain agriculture	Agricultural land
33	UA-2	Floodplain built-up area	Paved / Built-up area
34	UB-1	Floodplain forest	Natural forest
35	UB-2	Floodplain shrubs	Shrubs
36	UB-3	Floodplain production forest	Production forest
37	UG-1	Floodplain grass land	Natural grassland
38	UG-1-2	Floodplain grass land (natural or production)	Production / natural meadows
39	UG-2	Floodplain production grass land	Production meadows
40	UM-1	Natural levee or floodplain reed	Reeds and other helophytes
41	UR-1	Floodplain herbaceous vegetation	Herbaceous vegetation
42	V.1-2	Floodplain swamp	Herbaceous vegetation
43	VI.2-3	Softwood shrubs or pioneer softwood forest	Shrubs
44	VI.4	Softwood forest	Natural forest
45	VI.7	Floodplain willow production forest	Willow production forest
46	VI.8	Production forest on shoreline	Production forest
47	VII.1	Swampy inundation grass land	Natural grassland
48	VII.1-3	Swampy inundation grass land / structure rich grass land / production grass land	Production / natural meadows
49	VII.3	Production grass land	Production meadow

Table 2 Overview of uncertainty (expressed as the spread, i.e., the 68% confidence interval) in hydrodynamic and ecological model output due to errors in the land cover map according to two classification accuracies.

Model output		Waal	Nederrijn	IJssel
Water level (cm) ^a	69% CA	12 (8)	15 (9)	19 (12)
	95% CA	5 (3)	7 (5)	7 (5)
Discharge distribution (m ³ s ⁻¹) ^b	69% CA	89 (340)	85 (338)	65 (156)
	95% CA	58 (92)	49 (78)	37 (83)
Sediment deposition: 16 th and 84 th percentile (kg m ⁻² y ⁻¹)	69% CA	2.076-2.080	1.301-1.315	0.795-0.806
	95% CA	2.096-2.104	1.326-1.331	0.782-0.786
Ecotoxicological hazards ^c	69% CA	0.39-0.42	0.16-0.19	0.54-0.60
	95% CA	0.46-0.48	0.22-0.23	0.71-0.72
Ecotoxicological consistency ^d	69% CA	0.75	0.88	0.52
	95% CA	0.93	0.94	0.87
FI values: average normalized spread for habitat types	69% CA	0.27	0.28	0.28
	95% CA	0.11	0.33	0.23
FI values: average normalized spread for 29 species	69% CA	0.15	0.10	0.12
	95% CA	0.05	0.07	0.06

^a Maximum of the spreads, computed on the rivers kilometers per region; in brackets the median spread is given.

^b Spread of discharge variation per distributary, in brackets the range.

^c Values represent the fraction of little owl habitat with a daily cadmium intake exceeding a toxicity threshold of 148 µg d⁻¹.

^d Values represent the fraction of the little owl habitat that is either in 0, or in 15 of the realizations exceeding the toxicity threshold of 148 µg d⁻¹. Hence they represent the area where the ensemble gives consistent outcome.

Table 3 SEDIFLUX model output: distribution statistics (mean, 16% and 84% percentiles) of the annual sediment deposition (n = 15) in the Rhine branches and entire model area.

	Mean		16% percentile		84% percentile		spread	
	69%	95%	69%	95%	69%	95%	69%	95%
	CA	CA	CA	CA	CA	% CA	CA	CA
Entire model area								
Deposition flux density (kg m ² y ⁻¹)	1.43	1.44	1.43	1.44	1.44	1.44	0.008	0.002
Total annual deposition (tonnes y ⁻¹)	476	476	475	475	477	476	2	1
Bovenrijn								
Deposition flux density (kg m ² y ⁻¹)	1.32	1.29	1.31	1.28	1.33	1.29	0.018	0.009
Total annual deposition (tonnes y ⁻¹)	31	30	31	30	31	30	0.4	0.1
Waal								
Deposition flux density (kg m ² y ⁻¹)	2.26	2.29	2.25	2.29	2.26	2.30	0.008	0.010
Total annual deposition (tonnes y ⁻¹)	221	223	221	223	222	223	1	0.4
Nederrijn-Lek								
Deposition flux density (kg m ² y ⁻¹)	1.31	1.33	1.30	1.33	1.31	1.33	0.013	0.005
Total annual deposition (tonnes y ⁻¹)	135	137	135	136	136	137	1	0.5
IJssel								
Deposition flux density (kg m ² y ⁻¹)	0.80	0.78	0.80	0.78	0.81	0.79	0.010	0.004
Total annual deposition (tonnes y ⁻¹)	89	87	88	86	89	87	1	0.5

Table 4 BIO-SAFE codes for habitat types and description.

Habitat code	Description
H6120	Xeric sand calcareous grasslands
H6430_A	<i>Hydrophilous</i> tall herb fringe communities of plains with <i>Filipendula ulmaria</i>
H6430_B	<i>Hydrophilous</i> tall herb fringe communities of plains with <i>Epilobium hirsutum</i>
H6430_C	<i>Hydrophilous</i> tall herb fringe communities of plains along dry forests
H6510_A	Lowland hay meadows with <i>Alopecurus pratensis</i>
H6510_B	Lowland hay meadows with <i>Sanguisorba officinalis</i>
H91E0_A	Softwood alluvial forests with <i>Salix alba</i>
H91E0_B	Softwood alluvial forests with <i>Alnus glutinosa</i> and <i>Fraxinus excelsior</i>
H91F0	Riparian mixed forests of <i>Quercus robur</i> , <i>Ulmus laevis</i> and <i>Ulmus minor</i> , <i>Fraxinus excelsior</i> or <i>Fraxinus angustifolia</i>

Figure headings

Figure 1 Study area showing the three main distributaries of the river Rhine ; Bovenrijn-Waal, Pannerdensch Kanaal-Nederrijn-Lek and IJssel. At the bifurcation points "Pannerdensche Kop" and "IJsselkop" the water is distributed over the three branches.

Figure 2 Recoding of a polygon of the ecotope type 'High water free grassland' (ecotope number 7) based on the cumulative probability function for this ecotope type as derived from the map purities. With a random number of 0.71, the polygon is recoded into ecotope type 25, i.e. 'Natural levee or floodplain production grassland' for a 69% CA, whereas it remains nr 7, 'High water free grassland,' for a 95% CA.

Figure 3: Spatial distribution of model uncertainty for a section of the river IJssel: a) spread in water level (m) at a $16.000 \text{ m}^3\text{s}^{-1}$ discharge resulting from a 69% CA, b) same, but for a 95% CA, c) median of predicted annual average suspended sediment deposition ($\text{kg m}^{-2} \text{ y}^{-1}$), d) spread in annual average sediment deposition ($\text{kg m}^{-2} \text{ y}^{-1}$) due to a 69% CA, e) same, but for a 95% CA, f) nr of runs with the daily cadmium intake of the little owl exceeding a toxicity threshold of $148 \mu\text{g}$ cadmium per day for a 69% CA, g) same, but for a 95% CA.

Figure 4: Spatial distribution of model uncertainty for a section of the River Waal: Subpanels equal to Fig. 3.

Figure 5 The spread in water level at the river axis for the three distributaries. Both the median and the maximum spread correlate linearly with the discharge at the upstream boundary of the study area.

Figure 6 Distribution of the normalized spread (spread / mean) of the annual average suspended sediment deposition.

Figure 7 Distribution of the number of times a polygon exceeded the toxicity threshold of $148 \mu\text{g d}^{-1}$. Data are summarized per distributary. Note that the distribution for CA95 is more bimodal due to the smaller number of changes in the land cover map.

Figure 8 BIO-SAFE Floodplain Importance (FI) scores for the 20 most sensitive protected species in each of the Rhine branches.

Figure 9 BIO-SAFE Floodplain Importance (FI) scores for nine terrestrial habitat types in the Rhine branches. The 68% confidence interval is indicated by the black vertical lines. Habitat codes are described in Table 4.

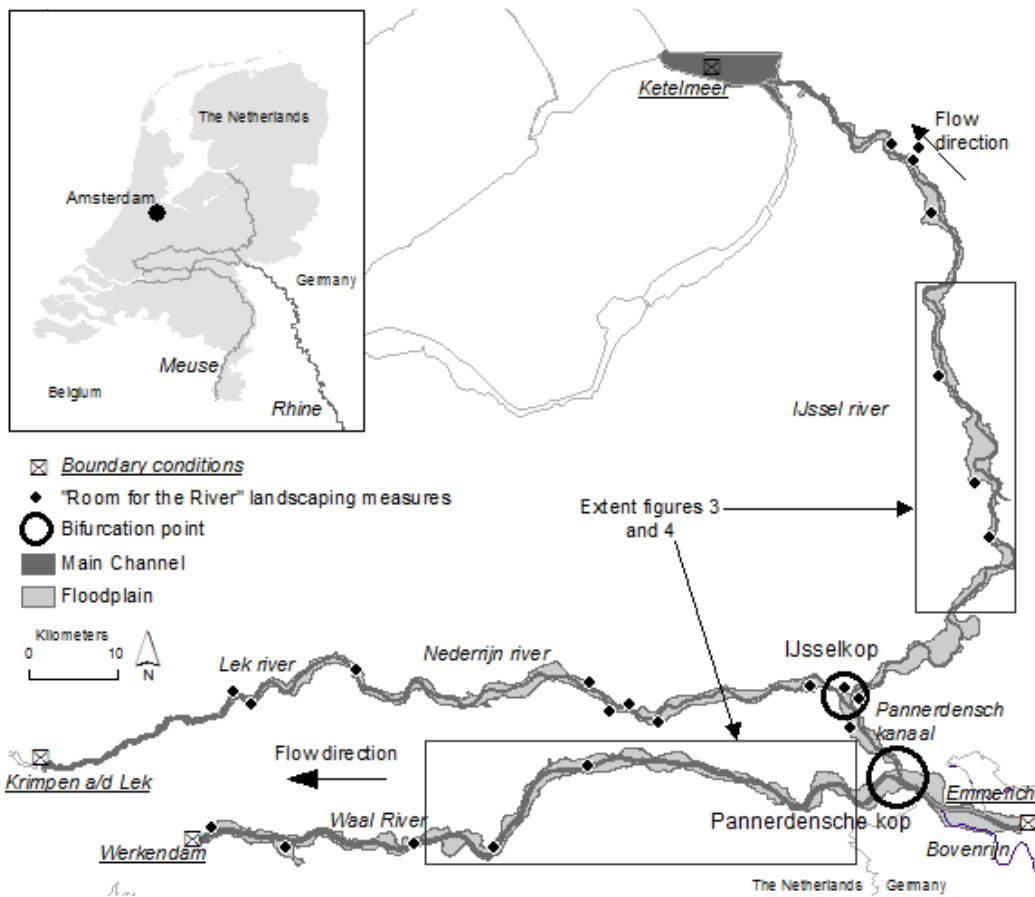


Figure 1

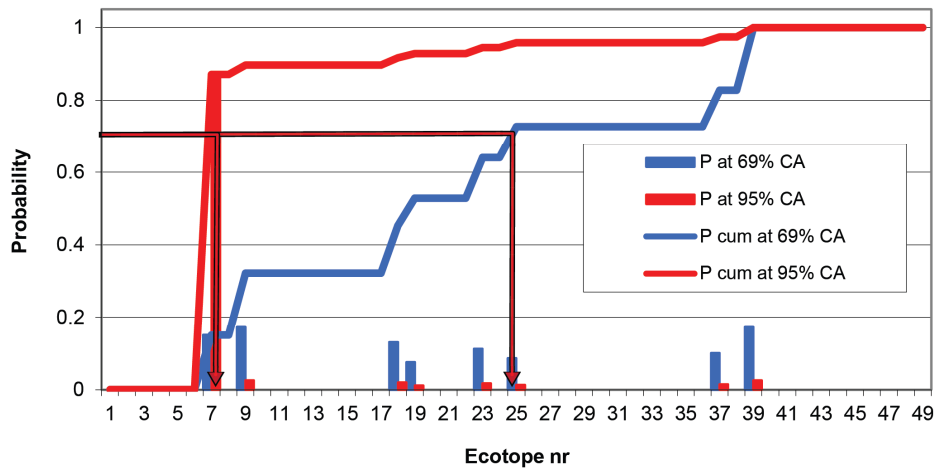


Figure 2

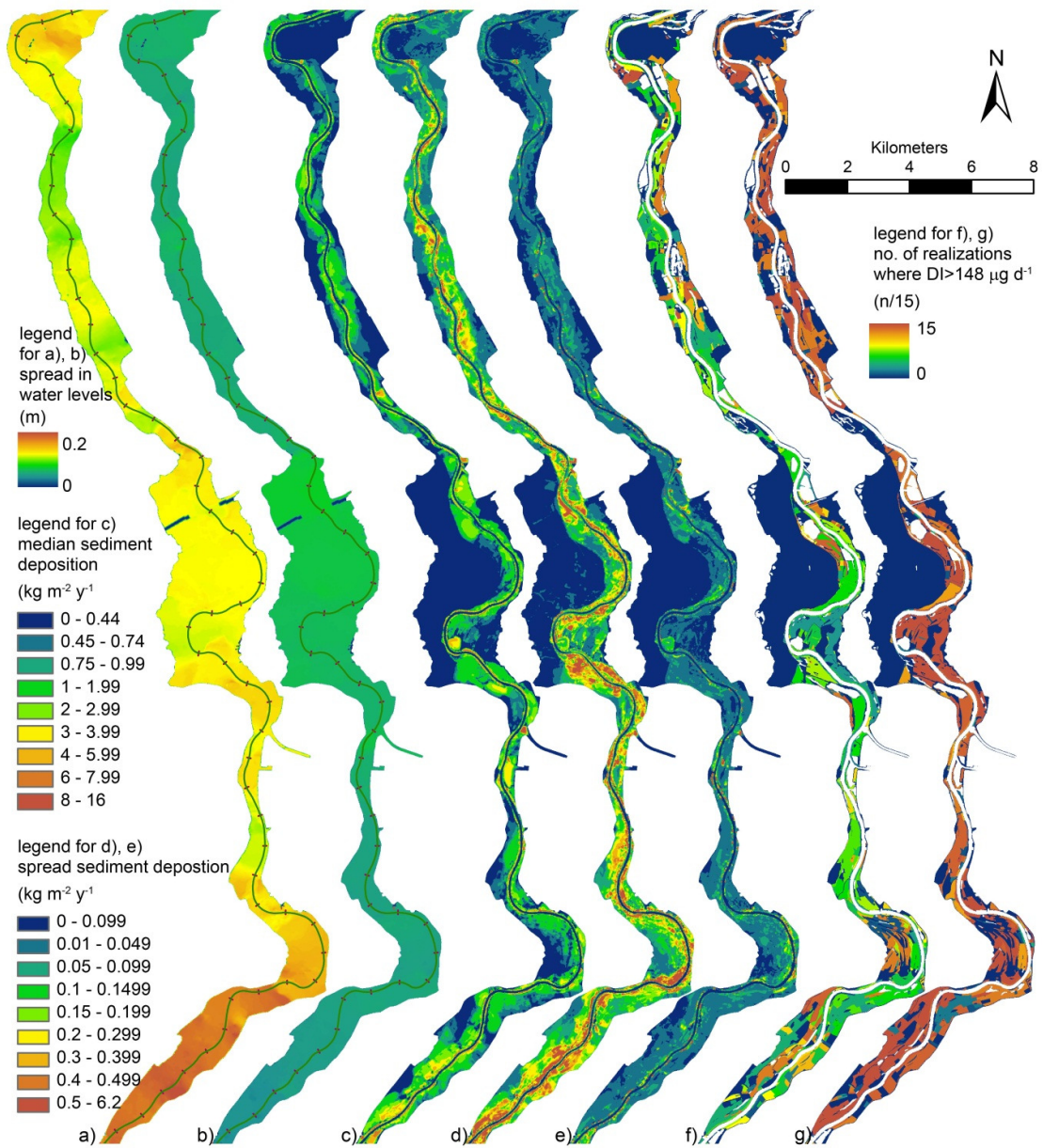


Figure 3

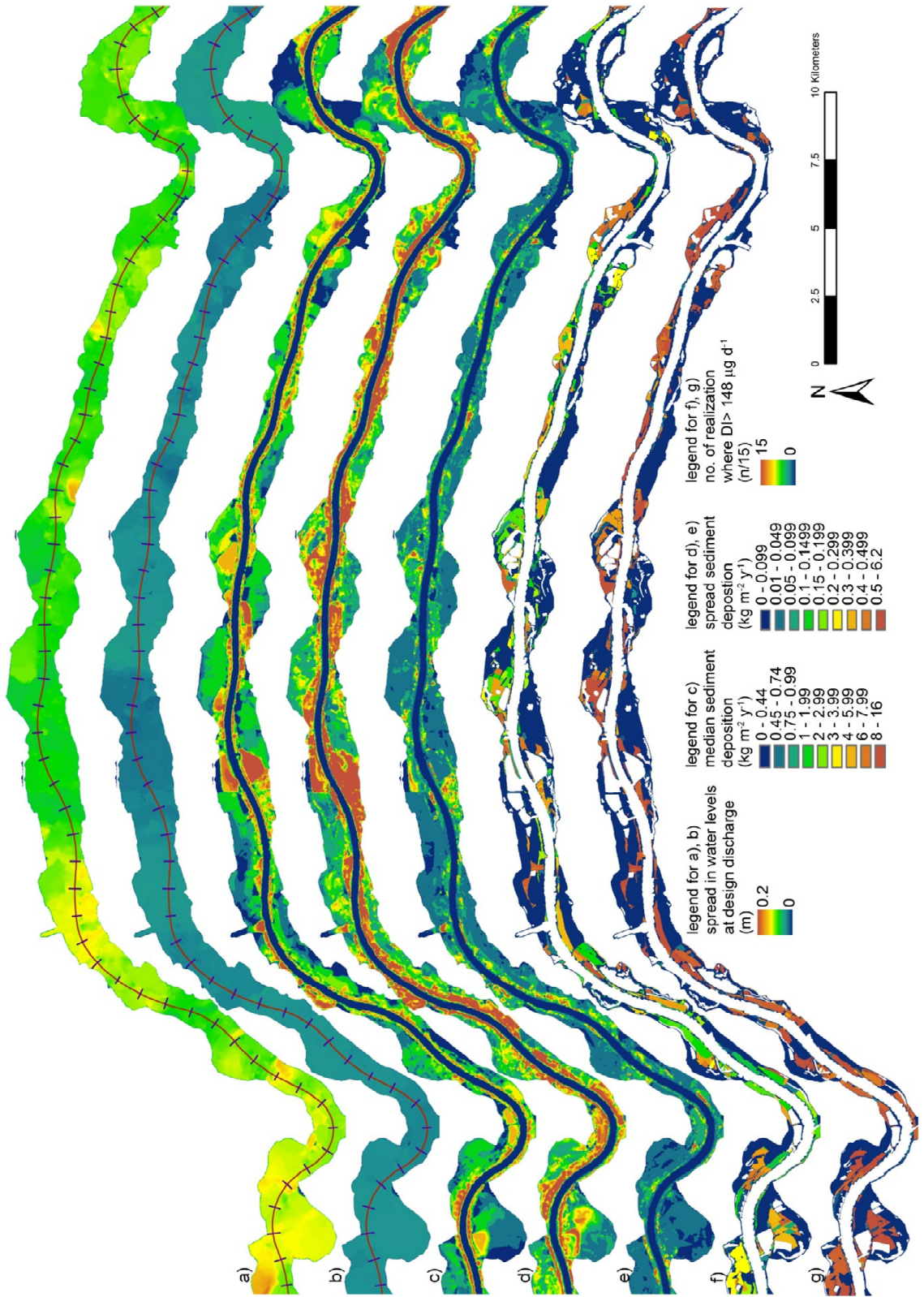


Figure 4

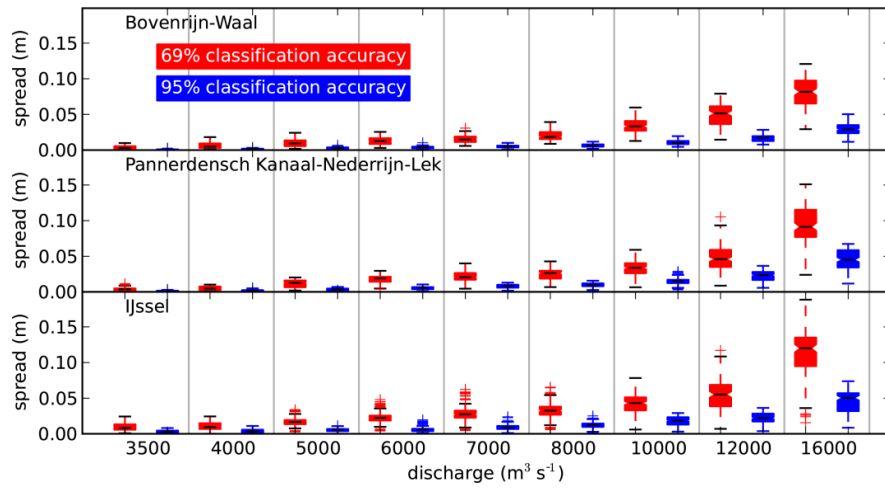


Figure 5

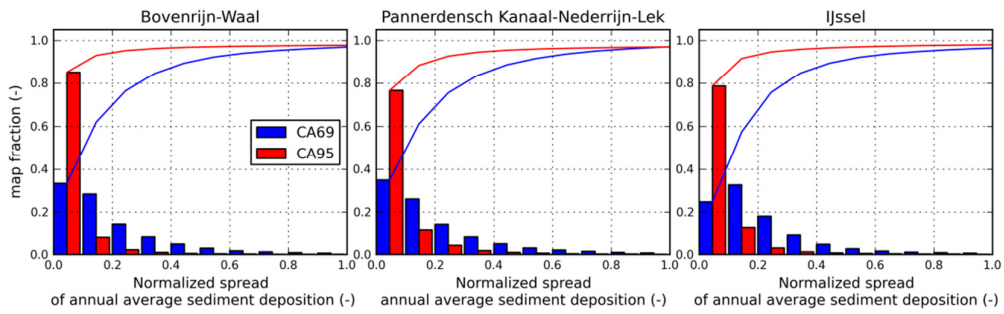


Figure 6

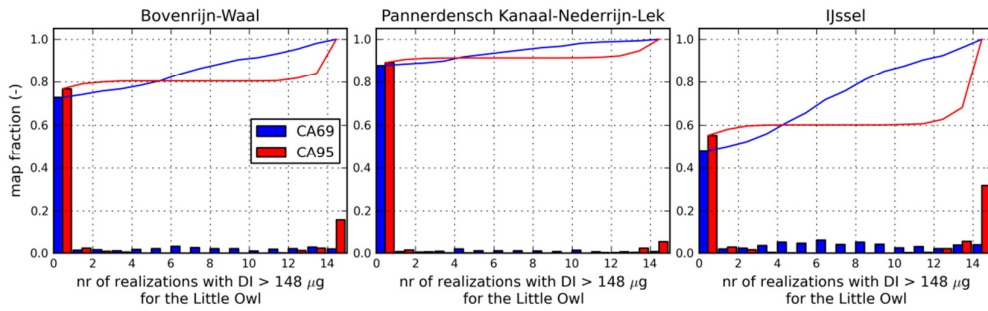


Figure 7

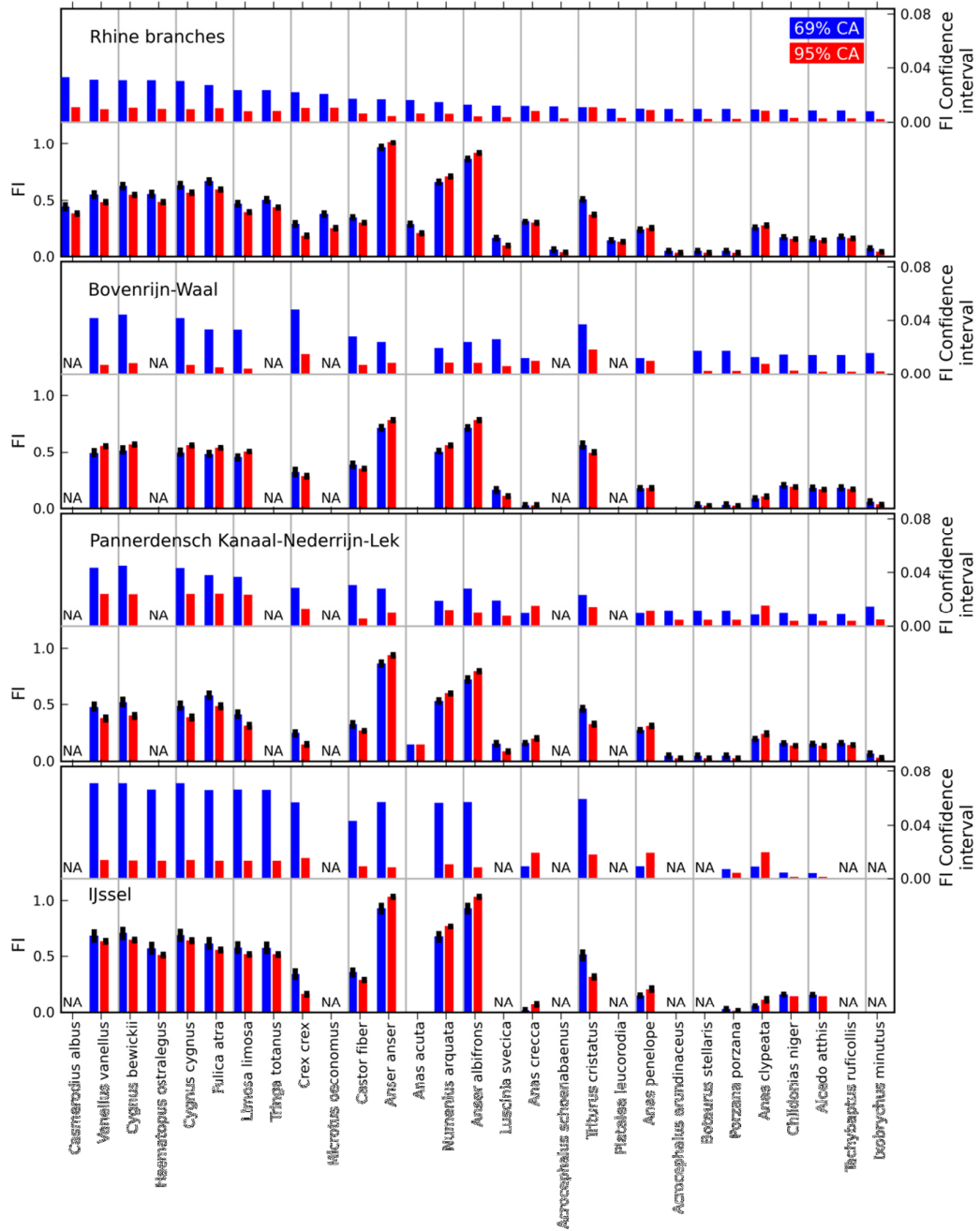


Figure 8

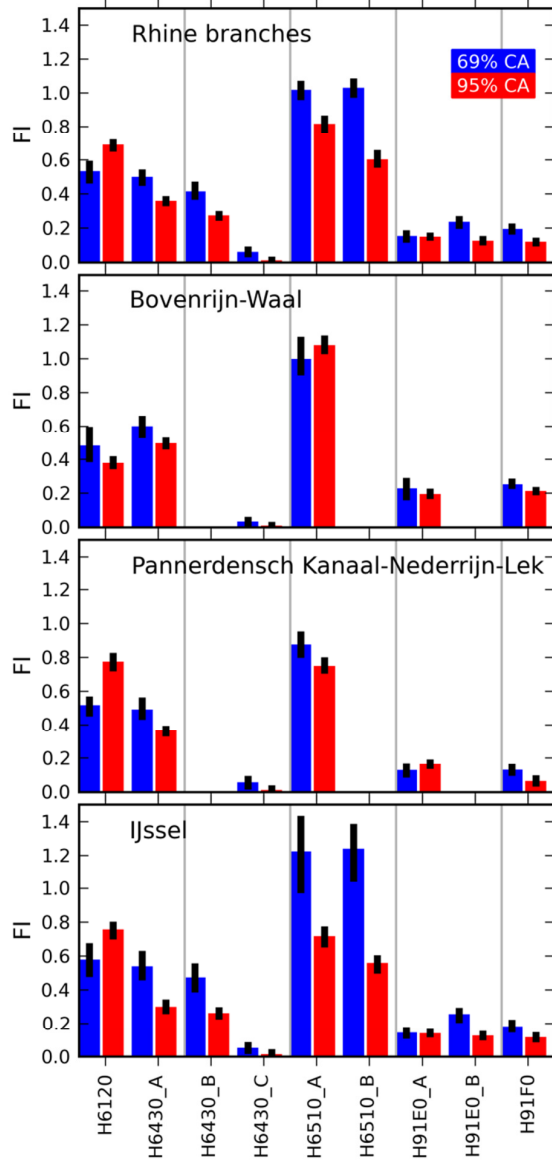


Figure 9